Impact Features on Stardust: Implications for Comet 81P/Wild 2 Dust

Friedrich Hörz, *et al.*

Science **314**, 1716 (2006);
DOI: 10.1126/science.1135705

system, the origin of silicate minerals around stars, and mixing in circumstellar disks. The mineral grains and components that we have seen in the comet are analogous to glacial erratics; they clearly did not form in the environment they were found in. Each particle is a treasure that provides clues on its place of origin and mode of transport. In many cases, it appears that they formed in the center of the solar nebula, and many of the larger particles are rocks composed of several minerals. Although better estimates will come from continued studies, initial investigations indicate that on the order of 10% or possibly more of the comet's mass was transported outward from the inner regions of the solar nebula as particles larger than a micron. The solar nebula may not have been well mixed, but the Stardust mission results show that there was abundant radial transport of solids on the largest spatial scales. One of the most surprising findings has been that we have seen many of these materials before. The distribution of minor element compositions of minerals, such as forsterite, indicate a link to the rare forsterite fragments found in primitive meteorites. Meteorite studies indicate that these high-temperature phases, serving as tracers, were distributed to varying degrees, sometimes as very minor components, across the inner parts of the solar nebula (*25*–*27*). From the work on Stardust samples, it now appears that components like forsterite and CAIs, formed in the hottest regions of the solar nebula, were transported over the entire solar nebula.

Comets have always been notable because of their contents of frozen volatiles but they are now additionally notable because of their content of exotic refractory minerals. The information on materials and mixing from the Stardust mission provide a new window of insight into the origin of solid grains that form disks around stars and lead to the formation of planetary bodies. This is a window that is explored with electron microscopes, mass spectrometers, synchrotrons, and a host of other modern instruments to provide information at levels of detail that were not previously imagined. The best available instruments and methods on the planet were used in this study, and it is expected that additional studies coupled with advances in analytical capabilities will continue to reveal important secrets about the origin and evolution of the solar system that are contained in these few thousand particles recovered from comet Wild 2.

References and Notes

1. D. E. Brownlee *et al.*, *Science* **304**, 1764 (2004).
2. Z. Sekanina *et al.*, *Science* **304**, 1769 (2004).
3. H. F. Levison, M. J. Duncan, *Icarus* **127**, 13 (1997).
4. D. R. Davis, P. Farinella, *Icarus* **125**, 50 (1997).
5. F. Horz *et al.*, *Science* **314**, 1716 (2006).
6. F. Horz *et al.*, *Icarus* **147**, 559 (2000).
7. G. Dominguez *et al.*, *Icarus* **172**, 613 (2004).
8. J. M. Greenberg, in *Comets*, L. L. Wilkening, Ed. (Univ. of Arizona Press, Tucson, 1982), pp. 131–163.
9. J. M. Greenberg, *Astron. Astrophys.* **330**, 375 (1998).
10. M. S. Hanner *et al.*, *Astrophys. J.* **425**, 274 (1994).
11. D. H. Wooden *et al.*, *Astrophys. J.* **517**, 1034 (1999).
12. F. Kemper, W. J. Vriend, A. G. G. M. Tielens, *Astrophys. J.* **609**, 826 (2004).
13. J. Dorschner *et al.*, *Astron. Astrophys.* **300**, 503 (1995).
14. D. Bockelée-Morvan *et al.*, *Astron. Astrophys.* **384**, 1107 (2002).
15. J. N. Cuzzi, S. S. Davis, A. R. Dobrovolskis, *Icarus* **166**, 385 (2003).
16. C. Lisse *et al.*, *Science* **313**, 635 (2006).
17. J. S. Mathis *et al.*, *Astrophys. J.* **217**, 425 (1977).
18. S. A. Sandford *et al.*, *Science* **314**, 1720 (2006).
19. Unequilibrated meteoritic materials have not experienced substantial diffusion of atoms between components, usually due to heating, that causes phases such as olivine to have the same elemental composition. The wide range of Fe/Mg ratios in Wild 2 olivine as well as the Ni content of sulfides show that the comet is at least as unequilibrated as the very rare and least equilibrated meteorites.
20. R. N. Clayton, *Nature* **415**, 860 (2002).
21. F. H. Shu *et al.*, *Astrophys. J.* **548**, 1029 (2001).
22. K. Okudaira, *36th Annual Lunar and Planetary Science Conference* **36**, 1832 (2005).
23. G. A. Graham *et al.*, *Dust in Planetary Systems*, Proceedings of the conference held 26 to 28 September 2005 in Kaua'i, Hawaii. LPI Contribution No. **1280**, 56 (2005).
24. C. Engrand *et al.*, *Meteoritics Planet. Sci.* **41**, 5237 (2006).
25. E. R. D. Scott, A. N. Krot, *Astron. Soc. Pacific Conf. Ser.* **341**, 15 (2005).
26. A. Pack, H. Palme, J. M. G. Shelley, *Geochim. Cosmochim. Acta* **69**, 3159 (2005).
27. S. Simon, L. Grossman, *Meteoritics Planet. Sci* **38**, 813 (2003).

28. The Stardust sample analysis team is grateful to NASA for funding and supporting the mission and to the hundreds of other team members that were involved in design, construction, flying, and recovery of the mission. The team, from 100 organizations, gratefully acknowledges their supporting institutions.

3 October 2006; accepted 17 November 2006
10.1126/science.1135840

REPORT

Impact Features on Stardust: Implications for Comet 81P/Wild 2 Dust

Friedrich Hörz,[1]* Ron Bastien,[2] Janet Borg,[3] John P. Bradley,[4] John C. Bridges,[5] Donald E. Brownlee,[6] Mark J. Burchell,[7] Miaofang Chi,[4] Mark J. Cintala,[1] Zu Rong Dai,[4] Zahia Djouadi,[3] Gerardo Dominguez,[8] Thanasis E. Economou,[9] Sam A. J. Fairey,[7] Christine Floss,[10] Ian A. Franchi,[5] Giles A. Graham,[4] Simon F. Green,[5] Philipp Heck,[11] Peter Hoppe,[11] Joachim Huth,[11] Hope Ishii,[4] Anton T. Kearsley,[12] Jochen Kissel,[13] Jan Leitner,[14] Hugues Leroux,[15] Kuljeet Marhas,[10] Keiko Messenger,[2] Craig S. Schwandt,[2] Thomas H. See,[2] Christopher Snead,[16] Frank J. Stadermann I,[10] Thomas Stephan,[14] Rhonda Stroud,[17] Nick Teslich,[4] Josep M. Trigo-Rodríguez,[18,19] A. J. Tuzzolino,[9] David Troadec,[20] Peter Tsou,[21] Jack Warren,[2] Andrew Westphal,[16] Penelope Wozniakiewicz,[12] Ian Wright,[5] Ernst Zinner[10]

Particles emanating from comet 81P/Wild 2 collided with the Stardust spacecraft at 6.1 kilometers per second, producing hypervelocity impact features on the collector surfaces that were returned to Earth. The morphologies of these surprisingly diverse features were created by particles varying from dense mineral grains to loosely bound, polymineralic aggregates ranging from tens of nanometers to hundreds of micrometers in size. The cumulative size distribution of Wild 2 dust is shallower than that of comet Halley, yet steeper than that of comet Grigg-Skjellerup.

Stardust's sample collector exposed SiO_2-based aerogel and aluminum foil to the flux of particles emanating from comet Wild 2 as the spacecraft's trajectory took it to within 234 km of the comet's surface (*1*). The cometary dust grains collided with these surfaces at 6.1 km s^{-1}, producing hypervelocity craters in the aluminum and deep penetration tracks in the highly porous, low-density aerogel (*2*) (fig. S1). Even the most cursory inspection of these surfaces reveals an unexpected diversity in the morphologies and sizes of both craters and tracks.

Detailed morphologic analysis of these impact features and comparison with experimental impacts produced by a suite of well-characterized projectiles was undertaken during the preliminary examination of Stardust to evaluate the common view that cometary solids are fluffy, highly porous objects (*3*). Also, the size distribution of Wild 2 dust can be deduced from the size distribution of the impact features and compared with those for other comets, such as Halley (*4*). In addition, attempts were made to analyze the compositions of molten projectile residues inside craters, as detailed by Zolensky *et al.* and Flynn *et al.* (*5*, *6*).

Stardust's fixed encounter speed of 6.1 km s^{-1} is well within the performance limits (~7 km s^{-1}) of small-caliber, light-gas guns, allowing direct laboratory simulation of Stardust's impact features (*7*–*9*). This is in stark contrast to earlier dust-collection experiments in low Earth orbit, which included aluminum (*10*) and SiO_2-based aerogel (*11*, *12*). Figure 1 compares experimental craters into Al_{1000} targets with those observed on Stardust foils and shows that detailed crater morphology reflects the physical properties of the impactor(s). It also illustrates

notable diversity among Stardust craters brought about by impactors that range from dense objects, such as nonporous silicates of ~3 g cm^{-3}, to highly porous aggregates with bulk densities as low as 0.3 g cm^{-3} (*8*). Detailed cross-sections through representative Stardust craters are shown in fig. S2 to quantify some of these morphologic characteristics, such as widely varying depth-to-diameter ratios and variable scales of surface roughness, which reflect particle density and structure.

We inferred the modal mineralogy of Wild 2 dust from the scanning electron microscopy (SEM) and energy dispersive spectrometer analyses of the molten residues in about 200 craters with diameters of <5 μm (Fig. 2A). Composite projectiles containing variable amounts of olivine, pyroxene, and Fe-sulfide are the most common (56%), and essentially monomineralic particles composed of primarily one of these three major phases make up an additional 36%. These major projectile types dominate at all crater sizes (Fig. 2B). Polymineralic impactors dominate even the smallest craters, some of which are <100 nm in size (Fig. 1F). This implies that individual components contributing to these tiny aggregates must be only tens of nanometers in size, finer than those of typical interplanetary dust particles (*13*). According to Kearsley *et al.* (*7*, *8*), most craters summarized in Fig. 2 are the result of submicrometer-sized impactors; all dust grains analyzed by Zolensky *et al.* and Flynn *et al.* (*5*, *6*) were an order of magnitude larger before impact. All analyses, however, suggest that small and large particles from Wild 2 are composed of a similar, if not identical, suite of minerals.

The penetration tracks in aerogel also displayed a wide range of morphologies. We distinguished three major groups: Type A tracks are carrot-like, with long, slender, continuously tapering walls. In contrast, type B tracks have more bulbous cavities, from which either one or a small number of slender tracks emerge, and resemble turnips with single or multiple roots. Type C tracks consist only of a bulbous, rather stubby cavity. We compared experimental tracks in aerogel formed at about 6 km s^{-1} with those from Stardust (Fig. 3). It seems evident from the laboratory simulations that the type A tracks were made by relatively cohesive impactors, whereas type B tracks resulted from poorly consolidated, fine-grained materials containing competent, coarse components. The fine-grained materials decelerate more rapidly and disperse radially with great efficiency to form a bulb, compared with the more massive and dense components that penetrate deeply. Alternatively, as illustrated by the lizardite experiment in Fig. 3C, the sudden release of copious volatiles could also contribute to bulb formation. However, there is no evidence to date for volatile rich materials in Wild 2 dust (*5*, *6*).

Quantitative measurements of the largest cavity diameter and maximum track length of all tracks in some 20 harvested tiles are illustrated in fig. S3. These measurements provide a quantitative basis for separating the three major track types, yet their transitions are highly gradational. These measurements also reveal that track morphology is size dependent: Most tracks less than 200 μm in length are type A, whereas most of the largest structures are type B; type C tracks are rare at all sizes.

In analogy to interstellar particles, small (<1 μm) and fluffy, highly porous particles are commonly thought to be typical for comets (*3*), but our observations indicate that such particles are only part of a broad continuum that also includes cohesive and dense objects. Particle size is highly variable as well and includes aggregates from <100 nm to >100 μm. This diversity in physical properties is unexpected for particles from a single comet, yet recent modeling of the light-scattering properties of the dust from comet Hale-Bopp also suggests a mixture of fluffy and dense particles (*14*).

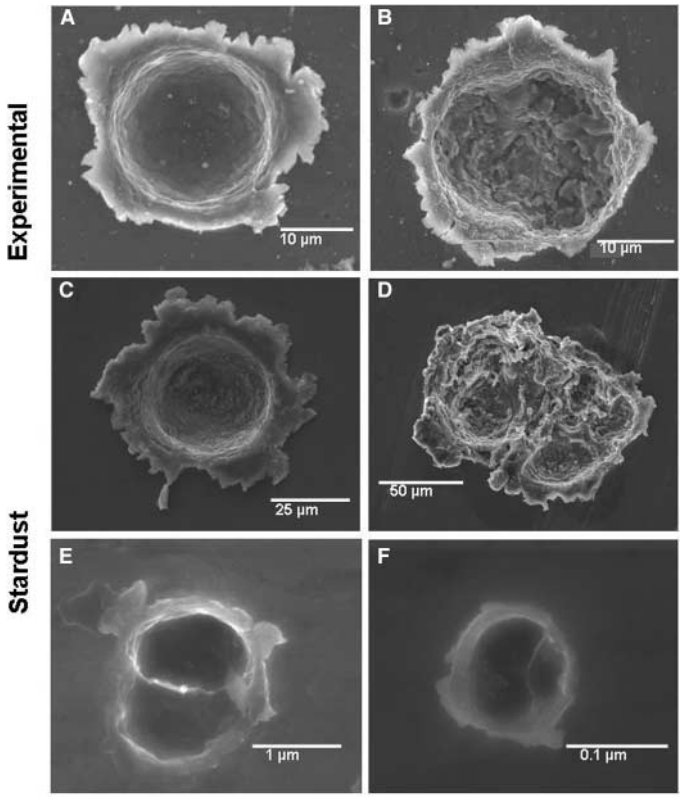

Fig. 1. Comparison of experimental craters (formed at ~6.1 km s^{-1}) and Stardust impacts. (**A**) Experimental crater made by a soda-lime glass sphere. (**B**) Experimental crater produced by an irregular fragment of powdered Allende meteorite. Notably, a crater's plan view grossly mirrors projectile shape. The physically homogeneous glass impactor produced a smooth floor, whereas the Allende crater is rugged, reflecting the fine-grained texture of Allende's matrix. (**C**) Fairly deep, bowl-shaped Stardust crater, suggestive of an equant, dense impactor [identified as Mg-rich silicate (*5*)]. (**D**) Compound, shallow Stardust crater characterized by irregular outlines and overlapping depressions that are separated by discrete septa. Such structures are the result of impactors with distinctly heterogeneous mass distributions, suggestive of aggregate particles with low bulk densities. Similarly, Stardust craters (**E**) and (**F**) are the products of aggregate impactors with discrete mass centers.

[1]Astromaterials Research and Exploration Science, NASA Johnson Space Center, Houston, TX 77058, USA. [2]Engineering Science Contract Group, NASA Johnson Space Center, Houston, TX 77058, USA. [3]Institut Astrophysique Spatiale, 91405 Orsay Cedex, France. [4]Institute for Geophysics and Planetary Physics, Lawrence Livermore National Laboratory, Livermore, CA 94550, USA. [5]Planetary and Space Sciences Research Institute, The Open University, Walton Hall, Milton Keynes MK7 6AA, UK. [6]Department of Astronomy, University of Washington, Seattle, WA 98195, USA. [7]Centre for Astrophysics and Planetary Sciences, University of Kent, Canterbury, Kent CT2 7NH, UK. [8]Department of Chemistry and Biochemistry, University of California San Diego, La Jolla, CA 92093–0356, USA. [9]Laboratory for Astrophysics and Space Research, Enrico Fermi Institute, University of Chicago, Chicago, IL 60637, USA. [10]Laboratory for Space Sciences, CB1105, Washington University, St. Louis, MO 63160–4899, USA. [11]Max Planck Institute for Chemistry, Particle Chemistry Department, Post Office Box 3060, 55020 Mainz, Germany. [12]Department of Mineralogy, The Natural History Museum, London SW7 5BD, UK. [13]Max Planck Institut for Solar System Research, 37191 Katlenburg-Lindau, Germany. [14]Institut für Planetologie, Westfälische Wilhelms-Universität Münster, 48149 Münster, Germany. [15]Laboratoire de Structure et Propriétés de l'Etat Solide, BAT C6, Université de Lille, F-59655 Villeneuve d'Ascq, France. [16]Department of Physics, University of California, Berkeley, CA 94720, USA. [17]Naval Research Laboratory, Code 6360, Washington, DC 20375, USA. [18]Institute of Space Sciences, Institut d'Estudis Espacials de Catalunya–CSIC, 08193 Barcelona, Spain. [19]Institut d'Estudis Espacials de Catalunya, 08034 Barcelona, Spain. [20]Insitut d'Electronique de Microélectronique et de Nanotechnologies, Université de Lille, F-59655 Villeneuve d'Ascq, France. [21]Jet Propulsion Laboratory, California Institute of Technology, Pasadena CA 91109–8099, USA.

*To whom correspondence should be addressed. E-mail: friedrich.p.horz@jsc.nasa.gov

Traywide scanning of all foils and aerogel surfaces at modest optical resolutions produced inventories of all large craters (with crater diameters $D_c > 20$ μm) and tracks (track diameters $D_t > 100$ μm) on the entire collector (*15*). The largest crater was 680 μm in diameter, and the widest track had a bulb diameter of 9.6 mm; the deepest track was 21.9 mm long. Their spatial distribution (fig. S4) suggests uneven, possibly nonrandom location of impact sites. In addition, detailed SEM analyses of individual foils reveal occasionally distinct clustering of craters (fig. S5). Similarly, individual aerogel cells show groups of small tracks that indicate distinctly off-normal trajectories, potentially representing secondary ejecta from the collision of dust with the upper surface of Stardust's collisional Whipple shield. However, none of the 250 craters and tracks analyzed by the entire preliminary examination effort indicates the presence of spacecraft debris (*5*, *6*, *16*). This raises the possibility that the observed clustering had natural causes. Particle fragmentation within cometary comae does not seem uncommon (*17*) and has been suggested specifically for Wild 2 (*18*) to explain the distinctly spiked impact rates observed by Stardust's Dust Flux Monitor Instrument (DFMI) (*19*). Current observations are insufficient to distinguish between these scenarios, and the projectile clustering on Stardust remains poorly understood.

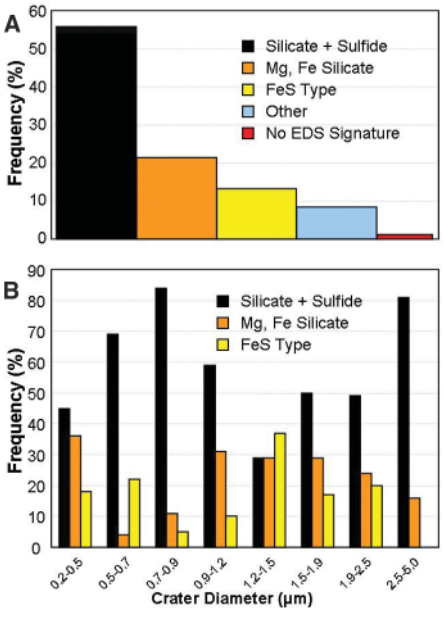

Fig. 2. Relative frequency of mineralogically distinct projectiles inferred from SEM and energy dispersive spectrometer analyses of projectile residues found as discontinuous and somewhat lumpy liners of shock-molten material on the floors and walls of Stardust foil craters. (**A**) Summary of all analyses. (**B**) Projectile composition as a function of crater diameter.

We next turned to the size frequency and fluence of Wild 2 dust based on the size frequency of craters and tracks and their areal density (number per square meter). The detailed crater and track counts are shown in fig. S6. The areal density of craters varies among individual foils by three orders of magnitude at $D_c > 10$ μm. The areal density of tracks varies as well, but only by one order of magnitude. This could relate to the scale of observation and integration, typically 8 cm^2 for individual aerogel tiles, but only 5 mm^2 (or less) for each foil. Regardless, the highly variable areal densities of both crater and tracks mandate a particle environment that is heterogeneous at scales ranging from millimeters squared to centimeters squared.

To obtain the size distribution of Wild 2 particles, we generated individual distribution curves for D_c and D_t that faithfully represent the relative size frequency of craters or tracks over the entire observational size range. Obviously, the traywide surveys define the large features, and the most thoroughly documented foils [8, 20, 37, and 52 (fig. S6)] and cells 12 and 23 were averaged for the small crater and track populations. These diameter data were then converted into spherical impactors (*20*). The results are plotted in Fig. 4. The independent crater and track calibrations seem to agree well for projectile diameters $D_p < 50$ μm, but they deviate at larger sizes. This is an artifact, because we assumed all measurements of D_t to be associated with type A tracks, akin to the experimental calibrations (*20*); bulbous track cavities most likely require smaller impactors than do carrot-shaped tracks at the same D_t, considering the pronounced, radial expansion of fine-grained materials. For this reason, we consider the crater-derived data more reliable at present.

A least-squares fit through the crater data only (inset in Fig. 4), results in a log-log slope of $D_p = -1.72$ and thus a mass slope of –0.57. This disagrees with the averaged slope of –0.85 for particles <50 μm measured by DFMI (*19*). However, the latter found large temporal and mass-dependent variations in this mass index from <–0.3 to –1.15 (*21*). The DFMI mass index of approximately –0.5 at $D_p > 50$ μm, including absolute fluence, is compatible with the collector observations, but we have no ready explanation as to why the two approaches produce seemingly discrepant results at the smaller sizes for comet Wild 2. The mass distribution of comet Halley (*4*) varies with particle size (and distance from the nucleus) but is steeper (~–1.0)

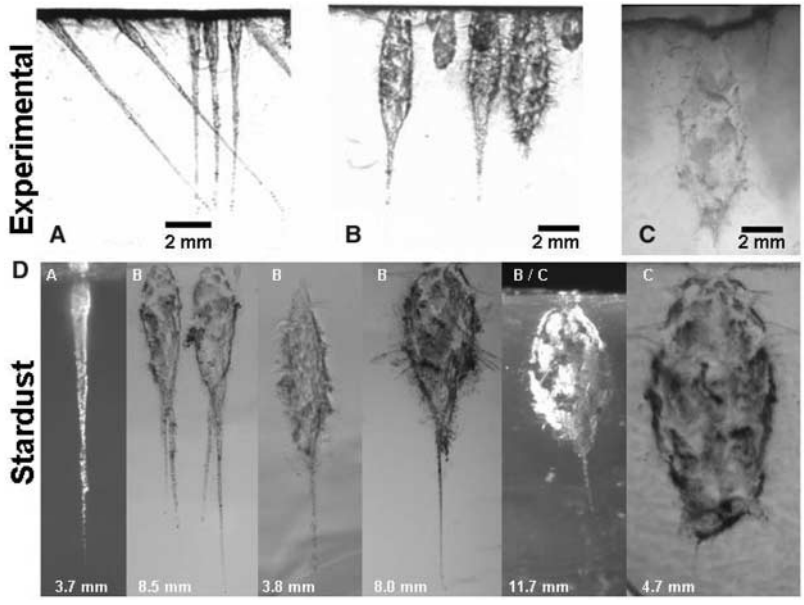

Fig. 3. Comparison of experimental aerogel tracks at 5 to 6 km s^{-1} with representative Stardust features. (**A**) Carrot-shaped tracks (type A) produced by two separate experiments, which used spherical glass projectiles that collided with the aerogel target at angles of 90° and 45° to the surface, thus demonstrating that tracks preserve some trajectory information. (**B**) Bulbous tracks resulting from glass projectiles embedded in a matrix of modestly compacted, very fine (cocoa) powder; the latter partly disaggregated during launch, producing poorly defined clods. Some of these clods contained glass beads that penetrated deeply to form slender termini (type B tracks), whereas others were composed of fine-grained powder only, resulting in type C tracks. (**C**) Bulbous track produced by a volatile-rich projectile (lizardite; containing 15% H_2O). (**D**) Stardust tracks that show, from left to right, the transition from slender (type A) to bulbous features with (type B) or without (type C) slender terminal portions. The total length of the Stardust tracks is given in millimeters.

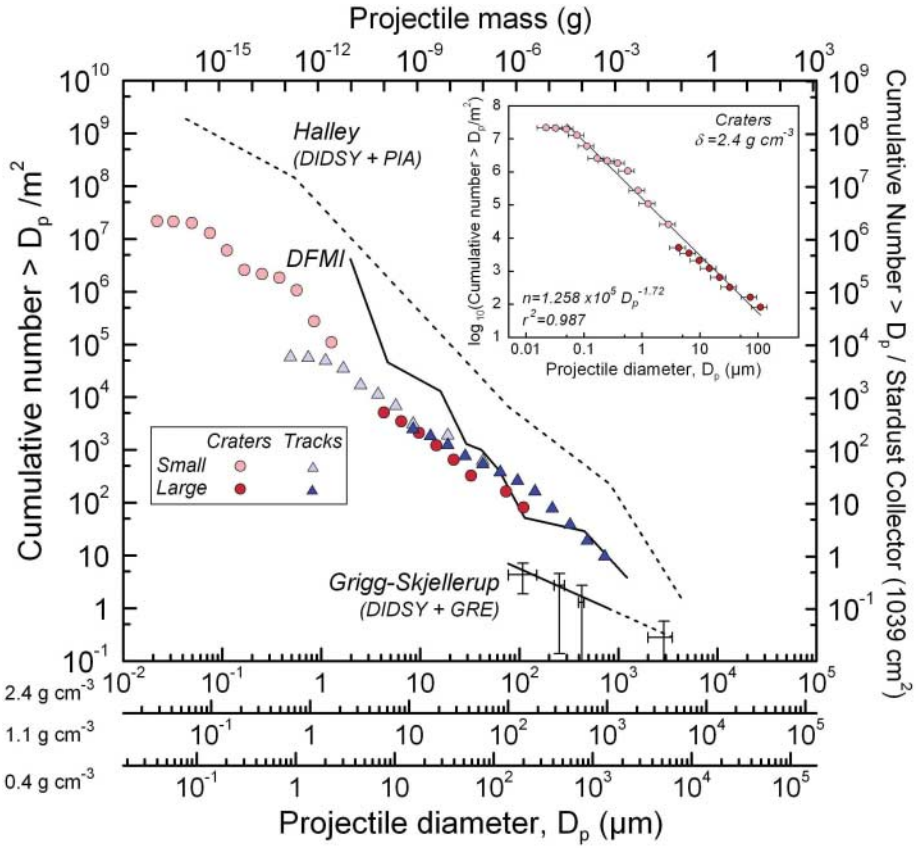

Fig. 4. Size distribution of Wild 2 dust, derived from the measurement of crater and track diameters (fig. S6) and impact calibration experiments (*7*, *20*) that used soda-lime glass (2.4 g cm^{-3}). The 1.1 and 0.4 g cm^{-3} scale bars apply only to craters (*8*), because current track calibrations are limited to soda-lime glass. Also plotted are the measurements of DFMI (*21*), which suggest a substantially steeper average slope than the collector observations. For comparison, in situ spacecraft observations for comets Halley [Dust Impact Detection System (DIDSY) and Particle Impact Analyzer (PIA)] (*4*) and Grigg-Skjellerup [DIDSY and Giotto Radio Science Experiment (GRE)] (*22*) are included. All spacecraft observations were modeled as spherical objects of 2.4 g cm^{-3}, and absolute fluence was adopted from Green *et al.* (*21*). (Inset) Least-square fit through all projectile diameter data, excluding the two points at the smallest sizes.

than that of Stardust over the region measured by both. Wild 2 dust thus seems deficient in small particles compared with that of Halley. The mass index for comet Griggs-Skjellerup, however, is –0.31 (*22*), at about D_p > 100 μm, suggesting fewer small particles than observed by Stardust.

Using the projectile size distribution and fluence of Fig. 4, we calculated a total mass of ~3 × 10^{-4} g of comet material that encountered the entire Stardust collector, yet the actual mission yield could be smaller as a result of impact-induced mass loss. Obviously, most mass is contained in only a few particles that are >100 μm, yet thousands of individual craters and tracks were retrieved that contain residues of Wild 2 dust massive enough to be analyzed individually by state-of-the-art instruments. Such analyses are just beginning.

References and Notes

1. D. E. Brownlee *et al.*, *Science* **304**, 1764 (2004).
2. Total exposed surface area was 1039 cm^2 for aerogel and 152 cm^2 for the Al foils (Al$_{1100}$; 100 μm thick).
3. J. M. Greenberg, A. Li, *Space Sci. Rev.* **90**, 149 (1999).
4. J. A. M. McDonnell, P. L. Lamy, G. S. Pankiewicz, in *Comets in the Post-Halley Era, Vol. 2*, R. L. Newburn *et al.*, Eds. (Kluwer Academic, Norwell, MA, 1991), pp. 1043–1073.
5. M. E. Zolensky *et al.*, *Science* **314**, 1735 (2006).
6. G. J. Flynn *et al.*, *Science* **314**, 1731 (2006).
7. A. T. Kearsley *et al.*, *Meteorit. Planet. Sci.* **41**, 167 (2006).
8. A. T. Kearsley *et al.*, *Meteorit. Planet. Sci.*, in press; preprint available at http://xxx.lanl.gov/abs/astro-phys/0612013.
9. M. J. Burchell *et al.*, *Annu. Rev. Earth Planet. Sci.* **34**, 385 (2006).
10. A. S. Levine, Ed., *LDEF—69 Months in Space, Third Post-Retrieval Symposium*, Williamsburg, VA, 8 to 12 November 1993 (NASA Conference Publication 3275, 1993).
11. F. Hörz, T. H. See, M. E. Zolensky, R. P. Bernhard, J. L. Warren, *Icarus* **147**, 559 (2000).
12. The impact velocities for these low Earth orbit instruments are basically unknown, but mean velocities are 15 to 17 km s^{-1} and thus beyond light-gas gun capabilities. Impact angles are random in low Earth orbit, but they were constant and normal to the collector surfaces for Stardust.
13. F. J. M. Rietmeijer, in *Planetary Materials*, vol. 36 of *Reviews in Mineralogy*, J. J. Papike, Ed. (Mineralogical Society of America, Washington, DC, 1998), pp. 2.1–2.95.
14. J. Lasue, A. C. Levasseur-Regourd, *J. Quant. Spectros. Radiat. Transfer* **100**, 220 (2006).
15. The collector-wide surveys are complete and included all craters with D_c > 20 μm (n = 63) and all tracks of D_t > 100 μm (n = 256). All SEM observations combined refer to a cumulative foil surface of <2 cm^2 (<2% of the collector surface); all detailed track data (e.g., fig. S3) refer to about 20 aerogel tiles, in part incomplete, and thus ~13% of the total aerogel collector surface.
16. S. A. Sandford *et al.*, *Science* **314**, 1720 (2006).
17. P. M. Edenhofer *et al.*, *Astron. Astrophys.* **187**, 712 (1987).
18. B. C. Clark *et al.*, *J. Geophys. Res.* **109**, 10.1029/2004JE002319 (2004).
19. A. J. Tuzzolino *et al.*, *Science* **304**, 1776 (2004).
20. All calibration experiments were conducted at 6.0 to 6.2 km s^{-1} and used projectiles 10 to 100 μm in size and Stardust "flight spare" Al foils and density-graded aerogel targets. Experiments by Kearsley *et al.* in (*7*) used spherical projectiles of soda lime-glass (2.4 g cm^{-3}), whereas polymethylmethacrylate (1.1 g cm^{-3}) and hollow glass spheres (0.4 g cm^{-3}) were used by Kearsley *et al.* in (*8*). Least-squares fits through the measured crater diameters (lip-crest to lip-crest) yielded the empirical constants K in the general relationship of $D_c = KD_p$. Corresponding experiments into Stardust aerogel are ongoing and presently limited to glass beads that produce carrot-shaped type A tracks (*23*); bulbous tracks remain uncalibrated, because they can be produced presently only by clods of fine-grained material of undefined size or mass.
21. S. F. Green *et al.*, *J. Geophys. Res.* **109**, 10.1029/2004JE002318 (2004).
22. J. A. M. McDonnell *et al.*, *Nature* **362**, 732 (1993).
23. M. J. Burchell, personal communication.

24. The encounter of comet Wild 2 by Stardust was the fourth flight project of NASA's Discovery Mission Program. Numerous individuals in government, academia, and industry contributed to the design, manufacture, launch, cruise, fly-by, and safe return of the payload to Earth. In addition, the research reported here was generously supported by our home institutions and national funding agencies.

Supporting Online Material

www.sciencemag.org/cgi/content/full/314/5806/1716/DC1
SOM Text
Figs. S1 to S6
References

29 September 2006; accepted 10 November 2006
10.1126/science.1135705